Table 1 Divergence loads for $\bar{C}_{RB}=1$, $\bar{C}_{RA}=0$, $\bar{C}_{TA}\doteq\infty$

No.	$\bar{C}_{TB}$	Critical load Nonconservative	Conservative	Sign of Ω^*
1	0.5	1.93	1.11	+
2	1	2.18	1.31	+
3	2	2.51	1.64	+
4	4	2.84	2.15	+
5	6	2.99	2.56	+
6	8	3.08	2.89	+
7	π^2	π	π	0
8	10	$3.142...>\pi$	3.18	−

following simple example. Consider a column for which $\bar{C}_{TB}=0$ and $\bar{C}_{RA}$, $\bar{C}_{TA}$, and $\bar{C}_{RB}$ are arbitrary constants different from zero and infinity. Corresponding to this case, the buckling equation resulting from Eq. (11) is the following:

$$\sin k+\frac{k}{\bar{C}_{RA}}\cos k+\frac{k}{\bar{C}_{RB}}=0 \tag{23}$$

This equation for $\bar{C}_{RB}=1$ and $\bar{C}_{RA}\to\infty$ admits only the trivial solution $k=0$. Consequently, this column is of the flutter type, and its critical load can be determined by using only the dynamic method. Similarly, for $\bar{C}_{RB}=1$ and $\bar{C}_{RA}>1.05$ the column is associated with a flutter type instability. In contradiction to the foregoing cases for $\bar{C}_{RA}=\bar{C}_{RB}=1$, the critical (smallest) load k_{cr} is equal to π; namely, the column is a divergence type system. Apparently, there is an infinite number of columns associated with the latter type of instability for $\bar{C}_{RB}=1$ and $\bar{C}_{RA}<1.05$.

Next, numerical results are presented in Table 1 giving a comparison between the divergence critical loads (Case D.) of a column under a follower force, and the respective conservative column. Thus, the critical loads k_{cr} and $\tilde{k}_{cr}$, the sign of $\Omega^*(k_{cr})$ for $\bar{C}_{RA}=0$, $\bar{C}_{TA}\to\infty$, and $\bar{C}_{RB}=1$, and various values of $\bar{C}_{TB}$ are given. It is clear that the column under a follower force can carry a greater load than that of the corresponding conservative system only if $\Omega^*(k_{cr})\geq 0$; otherwise, $k_{cr}<\tilde{k}_{cr}$. It is also shown that the sign of $\Omega^*(k_{cr})$ depends on the stiffness constants.

A particular case, where the instability mechanism of a fixed-elastically supported column under a follower load may change from flutter to divergence, and vice versa depending on the value of the stiffness constant, is presented by Sundararajan.[7] Another work of this author pertinent to this paper is given in Ref. 8. Finally, it should be noted that the lower bound theorem of Ref. 3 does not apply here.

References

[1] Herrman, G. and Bungay, R. W., "On the Stability of Elastic Systems Subjected to Nonconservative Forces," *Journal of Applied Mechanics*, Vol. 86, 1964, pp. 435-440.

[2] Plaut, R. H., "Determining the Nature of Instability in Nonconservative Problems," *AIAA Journal*, Vol. 10, July 1972, pp. 967-968.

[3] Leipholz, E. H., "Aspects of Dynamic Stability of Structures," *Journal of Engineering Mechanics Div.*, EM2, Vol. 101, 1975, pp. 109-124.

[4] Kounadis, A. N., Giri, J., and Simitses, J. G., "Divergence Buckling of a Simple Frame, Subjected to a Follower Force," *Journal of Applied Mechanics, Transactions of ASME*, 1978, Vol. 45, No. 2, pp. 426-428.

[5] Kounadis, A. N., "The Effects of Some Parameters on the Nonlinear Divergence Buckling of a Nonconservative Simple Frame," *Journal de Mécanique Appliquée*, Vol. III, No. 2, 1979, pp. 173-185.

[6] Panayotounakos, E. D. Kounadis, N. A., "Elastic Stability of a Simple Frame Subjected to a Circulatory Load," *Journal of Sound and Vibration*, Vol. 64, No. 2, 1979, pp. 179-186.

[7] Sundararajan, C., "Influence of an Elastic End Support on the Vibration and Stability of Beck's Column," *International Journal of Mechanical Sciences*, Vol. 19, 1976, pp. 239-241.

[8] Sundararajan, C., "On the Stability of Divergence Type Elastic Systems," *Developments in Theoretical and Applied Mechanics*, Vol. 7, 1974, pp. 475-482.

30012 J80-085
90005

Thermal Coupling of 2.8-μm Laser Radiation to Metal Targets

D. B. Nichols* and R. B. Hall†
The Boeing Aerospace Company, Seattle, Wash.

Introduction

THE response of metal targets to high-intensity laser radiation includes effects of target heating,[1] imparted momentum,[2] mass removal,[3] and the ignition of surface plasmas[4] with ionization of both atmospheric and target species;[5] all other target effects, however, are conditioned by the thermal coupling. In spite of a broad current interest in chemical lasers and their application, little is known experimentally about the thermal coupling of pulsed HF laser radiation to metals. Reported herein are coupling measurements throughout the incident fluence range 25-1400 J/cm².

An axially symmetric laser pulse incident on a planar target, described by a time-dependent irradiance $q_i(r,t)$ W/cm², results in an absorbed flux at the surface $q_a(r,t)$ W/cm². Integration over the time of the event gives incident fluence $e_i(r)=\int q_i(r,t)\,dt$ and absorbed fluence $e_a(r)=\int q_a(r,t)\,dt$ in J/cm². The total incident laser pulse energy in joules is $E_i=2\pi\int e_i(r)\,r\,dr$ and the total thermal energy deposited in the target $E_a=2\pi\int e_a(r)\,r\,dr$. The total thermal coupling coefficient is the fraction of incident laser pulse energy which is converted into thermal energy in the target, $\alpha=E_a/E_i$; this coefficient was measured in the present work. Time-integrated spatial dependence of coupling is expressed as local coupling $\alpha_r(r)=e_a(r)/e_i(r)$.

Laser pulses exceeding certain threshold irradiance and fluence requirements[4] ignite a surface plasma which enhances the thermal coupling to a metal target.[6] Model calculations as well as experiments have shown[7,8] the dependence of thermal coupling processes on the normalized pulse length $\hat{\tau}$. $\hat{\tau}$ is the ratio of the laser pulse length t_p to the time required for an acoustic disturbance of velocity c to cross the beam radius r_b.

$$\hat{\tau}=ct_p/r_b$$

When $\hat{\tau}$ is small (≈ 1) the local coupling coefficient $\alpha_r(r)$ is optimized because during the pulse the spatial development of the laser-supported absorption wave is limited to a region near the surface; for these conditions the energy transfer can be described by one-dimensional models.

This Note reports the utilization of the first HF-DF chemical laser delivering several hundred joules in a few microseconds, to investigate 2.8-μm thermal coupling. A first experimental requirement for spot size is that the surface

Received Aug. 10, 1978; revision received Sept. 9, 1979.

Index categories: Radiation and Radiative Heat Transfer; Lasers.

*Research Scientist.

†Principal Scientist.

plasma formation threshold be reached. Within that constraint, larger spot diameters give lower values of $\hat{\tau}$ and smaller spots give fluence values further above threshold. Most of the present work was carried out with a FWHM beam spot diameter $d_s = 0.47$ cm, giving a $\hat{\tau} = 9$ while permitting the investigation of incident fluences an order of magnitude above the plasma threshold.

Experimental Method

The Boeing photoinitiated pulsed chemical laser (PHOCL-10) used in this work has been described elsewhere.[9,10] The beam diagnostic methods and the particular far-field spatial profile used here were detailed in Ref. 4. The half-maximum contour of the spatial profile is well approximated by a circle with 0.47-cm diameter. The spatially integrated time profile has FWHM of 4 μs and total length of 8 μs. Variation of target-delivered beam energy was accomplished without changing the relative spatial profile and with little change of the relative time profile.

Thermal coupling coefficients were measured by direct calorimetry. The 1.59-cm-diam targets were 0.13-cm thick, with thermocouples spot-welded to the rear surface. Axial diffusion times were only a few milliseconds, and the radial equilibration times were measured. The whole-target heat increment was divided by the incident beam pulse energy to obtain the thermal coupling coefficient α. Special surface preparation such as sanding or polishing was avoided in order to obtain results representative of metals having practical surfaces. A new target was used for each laser shot. Test samples of larger diameter were used to show that the results were not limited by sample diameter.

Measured Thermal Coupling

The measured coupling coefficient α is plotted in Figs. 1 and 2 for aluminum, titanium, stainless steel, and nickel as a function of incident HF laser energy. Also shown are total pulse fluence and peak irradiance (maximum in both space and time). The irradiance scale is linear up to 200 MW/cm^2 due to a constant pulse length near 4 μs. Above 140 J energy the laser pulse length was decreased to about 3 μs at 220 J.

The incident energy scale has absolute uncertainty of $\pm 8\%$, the fluence scale $\pm 9\%$, and the irradiance scale $\pm 13\%$. The relative uncertainty of $\pm 9\%$ in α is dominated by cooling curve extrapolations ($\pm 8\%$), and the estimated absolute uncertainty in α is $\pm 15\%$.

At low energies the aluminum thermal coupling of Fig. 1 follows the low-intensity absorptance value of about 6%. At threshold the coupling increases by a factor of three. Thereafter, increasing incident energy enhances the propagation of a laser-supported detonation wave away from the target surface, resulting in decreasing total thermal coupling. Similar behavior is seen for the other metals. For each target material the coupling coefficient above threshold is represented very well by the simple analytic form $\alpha \sim E_i^{-1}$. This equation is shown in Fig. 1 and 2 as solid curves. Over the wide range of fluence 200-1400 J/cm^2 for these conditions, a constant amount of energy is deposited in the sample for a given material, independent of incident beam pulse energy.

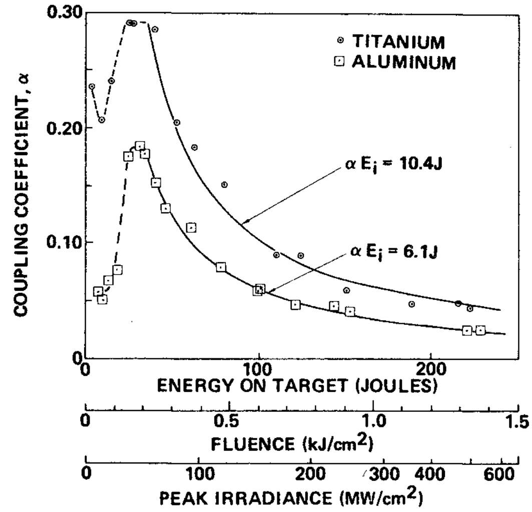

Fig. 1 Total thermal coupling of HF laser radiation on aluminum and titanium.

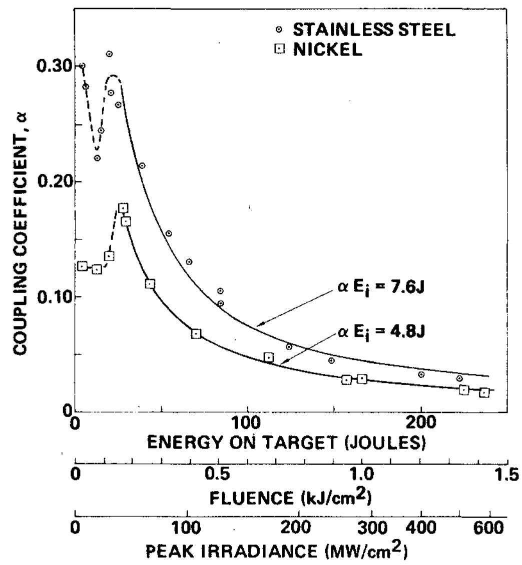

Fig. 2 Total thermal coupling of HF laser radiation on stainless steel and nickel.

The aluminum measurements were repeated at a few energy levels for a spot diameter of 0.94 cm to give comparative points for $\hat{\tau} = 4.3$. The largest coupling observed was $\alpha = 0.17$ at $e_i = 114$ J/cm^2.

Table 1 Measured thermal coupling parameters for pulsed HF laser radiation

Target material	Plasma formation threshold[a] (Ref. 4), J/cm^2	Thermal coupling enhancement threshold,[b] J/cm^2	Largest observed total coupling coefficient, α_{max}	Constant energy E_a deposited above threshold, J
Nickel	118	120	0.18	4.8
Aluminum 6061	120	120	0.18	6.1
Stainless Steel 321	96	95	0.29	7.6
Titanium[c]	84	95	0.29	10.4

[a]Effective beam spot diameter = 0.94 cm. [b]Incident-pulse fluence corresponding to threshold-step midpoint. [c]Commercially pure titanium (MIL-T-9046 Type I. Comp. B).

The thermal coupling enhancement thresholds apparent in Figs. 1 and 2 are compared in Table 1 to the corresponding thresholds for the formation of surface plasmas, taken from Ref. 4. There the plasma thresholds were measured for the same four metals and with the same laser, but with an effective beam spot diameter of 0.94 cm. The plasma thresholds listed in column 1 of Table 1 are the incident pulse fluence levels for which surface plasma ignition occurs halfway through the laser pulse. The largest observed coupling coefficients α_{max} and the constant energy deposited E_a are also tabulated. In Table 1 the material-dependent thermal coupling enhancement thresholds are clearly correlated with the material-dependent plasma formation thresholds. The lower thresholds (titanium and stainless steel) are associated with the higher values of α_{max} and the higher values of constant deposited energy $E_a = \alpha E_i$.

The variation of total thermal coupling to aluminum with ambient target pressure was measured for laser pulses of about 130 J. For air environment the coefficient α increased smoothly from 0.05 to 0.08 as pressure was reduced from 1 to 10^{-3} atm. The trend of decreasing α with increasing pressure is associated with the increasing density and shielding effect of the surface plasmas at higher ambient pressures.

Large differences in measured thermal coupling for cases of similar total incident fluences have been attributed to differences in the shape of the laser pulse time profile.[11] To investigate this effect, measured coupling coefficients were compared for pulse lengths 4 and 7 μs FWHM for both aluminum and titanium. There was no major shift in the thresholds due to this change of pulse length. The data above threshold were least-squares fitted to the power law $\alpha = aE_i^{-b}$. Short-pulse values of b were near unity for both metals in agreement with the overall E^{-1} dependence noted above. The long-pulse exponents of incident energy, $b = 0.84$ for aluminum and 0.70 for titanium, indicate that for the present conditions the long-pulse absolute energy deposited in the target continues to increase with incident energy even well above the plasma threshold.

Discussion

Two previous measurements of total coupling to aluminum at other wavelengths are notable because of the large focal spots used. Measurements at 1.06 μm by Hettche et al.[6] show a maximum $\alpha = 0.22$ for spot diameter of 0.56 cm ($\hat{r} \sim 7$). At 10.6 μm Marcus et al.[1] obtained values of α up to 0.33 on mechanically abraded targets for a spot diameter of 2.8 cm ($\hat{r} = 5.4$).

Certain reservations apply to all large-$\hat{r}$ measurement of total coupling. The radial spreading of the surface plasma can give contributions to the total coupling via target heating outside the beam spot.[12] This effect is minimized by minimizing $\hat{r}$, but the one-dimensional coupling, which is expected to scale to larger-spot conditions, is better indicated by spot-center measurements of local coupling $\alpha_r(0)$, which are insensitive to edge effects.

It should be noted, however, that the condition $\hat{r} \sim 1$ is not in itself sufficient to insure the "practical significance" of a thermal coupling measurement. Thermal effects depend on the energy fluence coupled to the target

$$e_a(r) = \alpha_r(r)\, e_i(r) = \alpha_r(r)\, q_i^{ave} t_p \tag{1}$$

where q_i^{ave} is an average incident irradiance. An optimized $\alpha_r(r)$ can be maintained at $\hat{r} = ct_p/r_b = 1$ by making t_p very short, but the useful e_a then approaches zero due to the small $e_i(r)$ in Eq. (1). A rough lower limit for a "useful" t_p may be set by using $\alpha_r(r) \leq 0.2$ and a usable $q_i^{ave} \leq 10^8$ W/cm^2 (due to axial decoupling as well as propagation limitations) to give the requirement $t_p \gtrsim 10^{-7}$ s.

Finally, the common assumption that $\hat{r} = 1$ is optimum should be used with care. If we minimize the incident pulse energy E_i required to deliver a specified absorbed fluence $e_a(r)$, several recent semi-empirical models of coupling data yield $2 < \hat{r} < 3$; that of Hall[13] gives $\hat{r} = 2.7$.

Acknowledgment

This work was supported by the U.S. Air Force Weapons Laboratory, Kirtland Air Force Base, New Mex., under Contract F29601-76-C-0030. The authors are indebted to L.A. Alexander Jr. for technical assistance.

References

[1] Marcus, S., Lowder, J.E., and Mooney, D.L., "Large-spot Thermal Coupling of CO_2 Laser Radiation to Metallic Surfaces," *Journal of Applied Physics*, Vol. 47, July 1976, pp. 2966-2968.

[2] Ferriter, N., Maiden, D.E., Winslow, A.M., and Fleck, J.A., "Laser-Beam Optimization for Momentum Transfer by Laser-Supported Detonation Waves," *AIAA Journal*, Vol. 15, Nov. 1977, pp. 1597-1603.

[3] Robin, J.E. and Nordin, P., "Effects of Gravitationally-Induced Melt Removal on CW Laser Melt-Through of Opaque Solids," *Applied Physics Letters*, Vol. 27, Dec. 1975, pp. 593-595.

[4] Nichols, D.B. and Hall, R.B., "Threshold Conditions for the Formation of Surface Plasmas by HF and DF Laser Radiation," *Journal of Applied Physics*, Vol. 49, Oct. 1978, pp. 5155-5164.

[5] Wei, P.S.P. and Nichols, D.B., "Spectroscopic Diagnostics of Laser-Supported Absorption (LSA) Waves Produced by a HF Laser," *Journal of Applied Physics*, Vol. 47, July 1976, pp. 3054-3056.

[6] Hettche, L.R., Tucker, T.R., Schriempf, J.T., Stegman, R.L., and Metz, S.A., "Mechanical Response and Thermal Coupling of Metallic Targets to High-Intensity 1.06-μ Laser Radiation," *Journal of Applied Physics*, Vol. 47, April 1976, pp. 1415-1421.

[7] Pirri, A.N., Root, R.G., and Wu, P.K.S., "Plasma Energy Transfer to Metal Surfaces Irradiated by Pulsed Lasers," *AIAA Journal*, Vol. 16, Sept. 1978, pp. 1296-1304.

[8] Boni, A.A., Su, F.Y., Thomas, P.D., and Musal, H.M., "Theoretical Study of Laser-Target Interactions," Science Applications Inc., LaJolla, Calif., SAI 77-567LJ, May 1977.

[9] Nichols, D.B., Hall, R.B., and McClure, J.D., "Photoinitiated $F_2 + H_2/D_2$ Chain-Reaction Laser with High Electrical Efficiency," *Journal of Applied Physics*, Vol. 47, Sept. 1976, pp. 4026-4030.

[10] Pond, C.R., Hall R.B., and Nichols, D.B., "HF Laser Spectral Analysis Using Near-Field Holography," *Applied Optics*, Vol. 16, Jan. 1977, pp. 67-69.

[11] Manlief, S.K., Mooney, D.L., and Marcus, S., "Repetitively Pulsed CO_2 Laser-Target Interaction," MIT Lincoln Laboratory, Lexington, Mass., LTP-34, Aug. 1976.

[12] Hall, R.B., Maher, W.E., Nelson, D.J., and Nichols, D.B., "High Power Laser Coupling," USAF Rept. AFWL-TR-77-34, 1977, pp. 78-81.

[13] Maher, W.E., Nichols, D.B., and Hall, R.B., "Three-dimensional Plasma Effects on Enhanced Thermal Coupling of Laser Beams," IEEE Conference on Plasma Science, Quebec, Canada, June 1979.

J 80 - 086

20014
70015
90011

Shock Tunnel Measurement of Ionization Rates in Hydrogen

R.J. Stalker*
University of Queensland, Australia

SIGNIFICANT nonequilibrium ionization may occur during atmospheric entry of probes to the outer planets,[1] and therefore knowledge of the rate of thermal ionization of

Received May 9, 1979; revision received Sept. 4, 1979.

Index categories: Thermochemistry and Chemical Kinetics; Reactive Flows; Entry Vehicle Testing, Flight and Ground.

*Professor, Dept. of Mechanical Engineering. Member AIAA.